

Flexible Metal–Organic Frameworks as CO₂ Adsorbents en Route to Energy-Efficient Carbon Capture

Xuan Yao, Kyle E. Cordova, and Yue-Biao Zhang*

Innovation in the realm of adsorbents for carbon capture is a necessity for meeting the carbon neutrality goal by 2060. Flexible metal–organic frameworks (MOFs) hold great promise for energy-efficient carbon capture as a direct result of their high working capacity, high selectivity, and intrinsic thermal management during gate-opening adsorption. In this review, the development and recent progress of flexible MOFs are summarized, the reported methods for control over flexibility are outlined, and the challenges and potential solutions of these materials toward practical carbon capture are discussed. It is envisioned that a deep molecular understanding of the adsorption mechanism in conjunction with a handle over gate-opening phenomena is a critical element for promoting the performance and large-scale application of flexible MOFs.


1. Introduction

According to the United States National Oceanic and Atmospheric Administration (NOAA), the concentration of CO₂ in the atmosphere exceeded 400 ppm in 2020,^[1] a primary contributor to the Earth, reaching its highest temperature rise of 1.1 °C.^[2,3] The Paris Agreement was signed to limit global warming by 2 °C (1.5 °C as the higher goal). If the global temperature rises 0.5 °C over the limit, the number of people suffering from water shortage would double and if the temperature rises another 0.5 °C, a number of insect species for crop pollination would become extinct and food shortage would occur worldwide.^[4] Aside from reducing emission from conventional energy consumption,^[5] an alternative approach is to capture CO₂ from point-source emission in a similar manner as to what happens directly from the atmosphere by vegetation and hydrology

X. Yao, Y.-B. Zhang
School of Physical Science and Technology
ShanghaiTech University
393 Huaxia Middle Rd, Pudong, Shanghai 201210, China
E-mail: zhangyb@shanghaitech.edu.cn

X. Yao, Y.-B. Zhang
Shanghai Key Laboratory of High-resolution Electron Microscopy
ShanghaiTech University
Shanghai 201210, China

K. E. Cordova
Materials Discovery Research Unit
Advanced Research Centre
Royal Scientific Society
Amman 11941, Jordan

 The ORCID identification number(s) for the author(s) of this article can be found under <https://doi.org/10.1002/ssr.202100209>.

DOI: 10.1002/ssr.202100209

systems every day. As the CO₂ content in industrial exhaust (e.g., associated gas and flue gas) is typically higher than what is found in the atmosphere, there is a need to develop chemical and material technologies for increasing the efficiency of carbon capture.

For traditional liquid absorption methods of carbon capture, dilute alkali solutions, such as monoethanolamine or mixed KOH/K₂CO₃ solutions, are used to absorb CO₂, and then CO₂ is regenerated through heating.^[6] During the regeneration process, the energy consumption is high, which leads to increased costs and extra energy serving as the basis for additional CO₂ emission. According to a report

in 2018, when CO₂ is delivered at 15 MPa, the design requires either 8.81 GJ of natural gas, or 5.25 GJ of gas, and 366 kWh of electricity, per ton of CO₂ captured.^[6b] At the same time, the equipment corrosion problem created by alkali solutions accelerates its aging, which again causes extra cost. To solve the problems existing for alkali adsorbents, solid adsorbents are recommended to prevent equipment corrosion, and there have been solid-state chemisorption materials such as amine-modified mesoporous silica proposed for use.^[7] On the other hand, physical adsorption usually requires lower energy change than chemical absorption, which means that it is not necessary for an extra energy supply for cooling the materials when capturing and heating them at the stage of CO₂ regeneration.^[8] Therefore, the solid physical adsorbents can lead to a safer, cheaper, and more environmentally friendly way for carbon capture.^[9] Zeolites are typical solid CO₂ physical adsorbents known for their high adsorption affinity,^[10] but their performance in the presence of atmospheric moisture and the energy consumption for CO₂ regeneration is unsatisfactory. By the end of the 20th century, the rise of reticular chemistry prompted the rational synthesis of porous materials and as a result, thousands of metal–organic frameworks (MOFs) were reported.^[11] The heat during gas adsorption on MOFs is typically lower than zeolites, and due to their rational synthesis, MOFs have been developed as effective and selective adsorbents under humid conditions,^[12] which positions them to a better choice for carbon capture than zeolites.^[13] In addition, MOFs can also be designed as catalysts to CO₂, which provide the possibility for sequential carbon capture and conversion.^[14]

There are various strategies for carbon capture from CO₂/N₂/CH₄ gas mixture using porous materials. First, given the smaller dynamic diameter of CO₂ molecules compared with most other gases, a good method for direct air capture (DAC) and

low-pressure flue gas is to narrow the pore size so that the porous materials adsorb CO₂ selectively.^[15] This is similar to the molecular sieve effect, which means that ultramicroporous materials like SIFSIXs are widely studied.^[16] Also, as the interaction of CO₂ molecules directly with the aperture walls of the framework materials is usually stronger than others, another choice is to enhance the interaction with CO₂ by introducing functional groups to the organic linkers of MOFs like amine or carboxyl groups.^[17] Furthermore, there can be open metal sites in some MOFs, which can provide a powerful CO₂ adsorption site close to chemical adsorption.^[18]

The working conditions of different types of carbon capture technologies requires different design methods for MOFs. For DAC, the CO₂ uptake at a partial pressure of 0.4–1 mbar is quite important and the competitive adsorption of water and CO₂ must be solved. For postcombustion capture, similar to DAC, satisfactory uptakes of CO₂ at low partial pressure and hydrophobicity are needed. For precombustion capture, the influence of water is weaker as the pressure is usually high, while the demand in working capacity and selectivity is higher. However, on the premise of restraining the regeneration energy consumption, the question arises of how to balance the working capacity and selectivity. If large gas uptake is undifferentiated, selective adsorption can be difficult. Researchers have made great strides in solving this problem by controlling the structure of MOFs to fabricate them with narrow channel windows for large selectivity and pore volume for large capacity, such as the case of JNU-3.^[19] The rational design of MOFs embodying such standards is not easy, and other universal methods remain needed. With the rise in circular carbon economy, balancing the carbon regeneration energy consumption, working capacity, and selectivity of MOFs is quite difficult.

Flexible MOFs are a class of MOFs featuring structural transformation upon external stimuli, such as guest inclusion, heat, pressure, or illumination.^[20] Before and after phase transformation, the pore structure and the adsorption properties of a flexible MOF will change; therefore, the flexibility (especially reversible flexibility) can be divided into many types, including breathing, swelling, and interpenetration displacement.^[21–23] Under appropriate stimuli, flexible MOFs can exhibit both high selectivity and working capacity with the change of structure and aperture. Furthermore, framework expansion during phase transformation is usually endothermic, so heat released during adsorption that typically disturbs adsorption performance can be neutralized, which is called intrinsic thermal management.^[24] Put simply, flexible MOFs can balance the three crucial standards for carbon capture, working capacity, selectivity, and energy consumption cost, which meet the requirements for precombustion capture. In addition, for some hydrophobic flexible MOFs with lower pressure of structure transformation, the flue-gas capture properties are also promising.

2. Gate-Opening Adsorption for Higher Working Capacity

Gate-opening adsorption is typically used to describe the adsorption performance of specific gases in flexible MOFs. When the partial pressure of a given adsorbate gas is below a threshold

value, flexible MOF structures contract, resulting in low uptake. Upon increasing the partial pressure, the structure then transforms to an open phase, leading to enhanced uptake. In most cases, the increase in uptake can be sudden; thus, when the working pressure condition is close to the threshold value, the usable working capacity will be larger than rigid frameworks that have similar uptake capacity.

Kaneko and co-workers reported a MOF termed ELM-11 ([Cu(BF₄)₂(4,4'-bipyridine)₂]_n).^[25] The MOF achieved gate-opening adsorption to N₂, CO₂, and Ar (Figure 1b). The authors attributed gate-opening adsorption to the interaction of hydrogen bonds. Kanoh, Kajiro, and co-workers observed expansion at a macroscopic crystal level corresponding to CO₂ adsorption. When the partial pressure of CO₂ reached 34.7 kPa at 273 K, an abrupt volume increase occurred to the MOF packed in a cell (Figure 1e).^[26] Later in 2011, the authors also reported a method to regulate the gate pressure through changing the pretreatment solvent and the temperature for activation, which suggested that ELM-11 has a different flexible response under different conditions (Figure 1c).^[27] Kaskel, Bon, and co-workers developed in situ powder X-ray diffraction (PXRD) measurements during CO₂ and butane adsorption at 273 K. A change in the PXRD patterns was observed and the partial pressure of the adsorbates is in accordance with the gating pressure according to the adsorption isotherms. After aligning the CO₂ adsorption isotherms at 273 and 195 K, it is obvious that aside from the gating pressure of the observed structural transformation, another step of adsorption occurs under a partial pressure of ≈0.3, which suggests that second gate-opening adsorption accompanied with structural transformation exists (Figure 1d).^[28] Kanoh and co-workers observed the double-step structural transformation and gate-opening adsorption of ELM-11 from both PXRD patterns and CO₂ adsorption isotherms at 195 K. Different PXRD patterns of ELM-11 were acquired at the gating pressure according to the CO₂ adsorption isotherms, and the PXRD pattern of the structure after the second step is quite similar with the pattern calculated for the CO₂-adsorbed structure at the same pressure (Figure 1g). The report also indicated that interlayer expansion occurs twice in sync with gate-opening adsorption.^[29]

C. Serre, G. Férey, and co-workers reported MIL-53-Cr (Cr(OH)(bdc), bdc = benzenedicarboxylic acid) as a water-stable Cr-based MOF that exhibits a very large breathing effect.^[30] This breathing effect was observed when the MOF adsorbed water molecules, in which the framework shrinks and the pore size decreases (Figure 2a). Furthermore, the authors reported different adsorption behaviors for CO₂ and CH₄ with the hysteresis of CO₂ adsorption isotherms, proving that the flexibility of MIL-53-Cr can also be triggered by CO₂ at high-pressure conditions.^[31] To enhance the selectivity, MIL-53-Cr was pretreated by hydrating the internal pore environment. This enabled MIL-53-Cr to prohibit the entrance of nonpolar molecules, such as CH₄, without impacting the step response of CO₂ over 1 MPa (Figure 2b).^[32] In practical application scenarios, MOFs will be compacted in a bed-type system where a gas mixture can be introduced thereafter. The selective adsorption of CO₂ by the chosen MOF will lead to a pure CO₂-free outlet. Researchers usually simulate the situation through dynamic breakthrough experiments, in which the flow rate and gas flow pressure into the MOF bed can be controlled and the off gas can be analyzed with an online

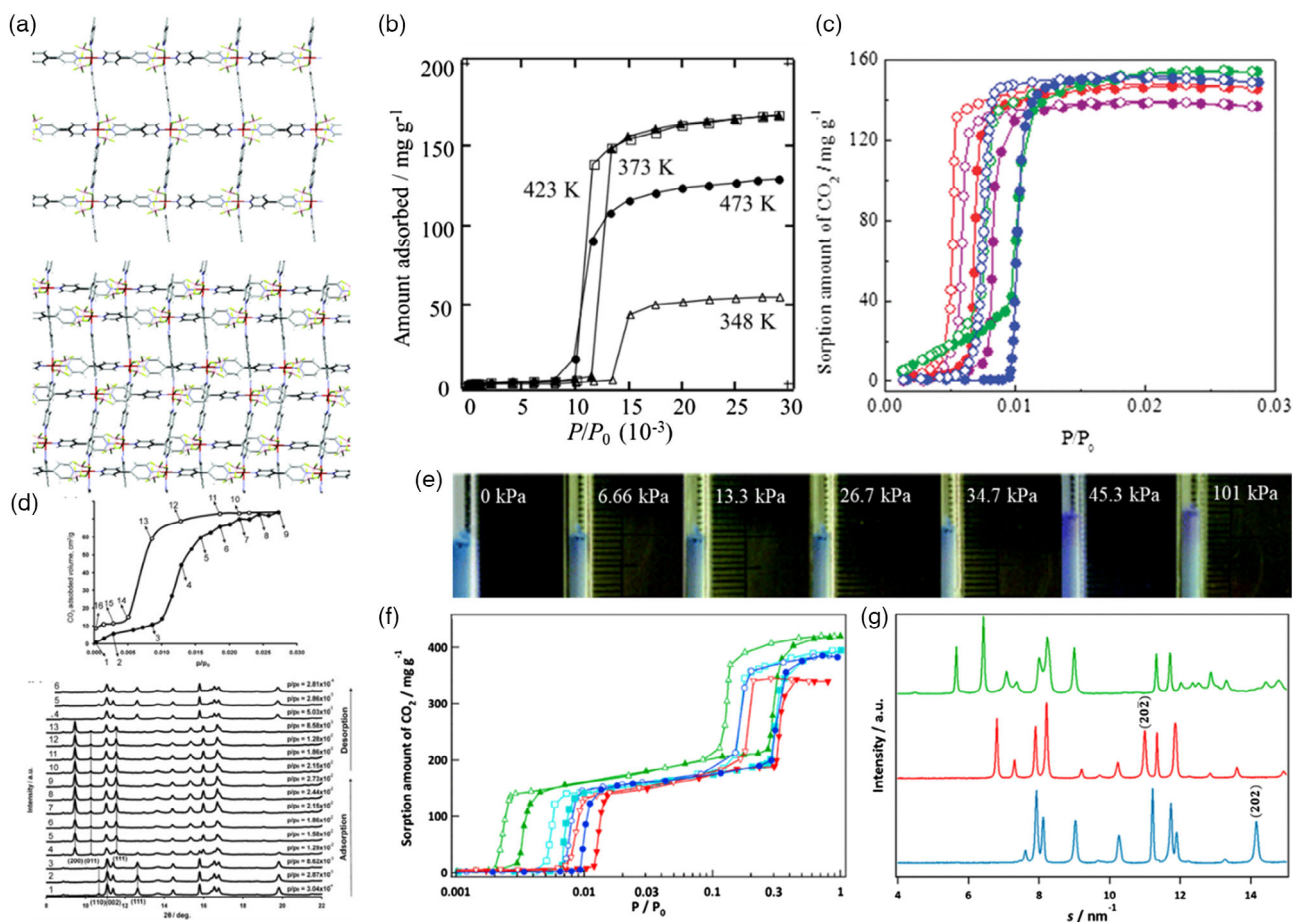


Figure 1. a) 2D sheet structure (up) and stacking structure (bottom) of ELM-11. b) Adsorption behavior of CO₂ on ELM-11 at 273 K pretreated at different temperatures. c) Adsorption isotherms of CO₂ at 273 K on activated ELM-11 (blue) and activated ELM-11 pretreated with methanol, ethanol, and propanol (purple, red, and green, respectively). d) In situ PXR patterns of ELM-11 corresponding with CO₂ adsorption at 273 K. e) Expansion of the volume of ELM-11 at the macroscopic crystal level with adsorption of CO₂ at different partial pressures. f) CO₂ adsorption isotherms of ELM-11 (semilog plot) measured at different temperatures (green, 195 K; light blue, 253 K; blue, 273 K; red, 298 K). g) PXR patterns of ELM-11 at 195 K (blue, after pretreatment [$P/P_0 = 0.001$]; red, after the first step [$P/P_0 = 0.013$]; green, after the second step [$P/P_0 = 0.60$]). a,e) Reproduced with permission.^[25] Copyright 2006, American Chemical Society. b) Reproduced with permission.^[26] Copyright 2001, Elsevier. c) Reproduced with permission.^[27] Copyright 2011, American Chemical Society. d) Reproduced with permission.^[28] Copyright 2014, Elsevier. f,g) Reproduced with permission.^[29] Copyright 2016, American Chemical Society.

gas chromatograph or mass spectrometer. To overcome the co-adsorption of CO₂ and CH₄ during the breakthrough measurement of MIL-53, the authors controlled the gas mixture's molar ratio and test pressure. Accordingly, a change in the breakthrough curve shape indicated adequate separation capabilities of MIL-53-Cr under prescribed working conditions (Figure 2c).^[33] Around the same time, Denayer and coworkers functionalized the linker used to construct MIL-53-Al with amino functional groups. Subsequent adsorption isotherms demonstrated that MIL-53-Al-NH₂ achieved better selectivity due to the material's higher affinity toward CO₂. Indeed, breakthrough measurements confirmed that MIL-53-Al-NH₂ excelled in the dynamic separation of CO₂/CH₄ (Figure 2d).^[34]

Kitagawa and co-workers reported a 2D MOF, [Cu₂(dhbc)₂(bpy)]_n (where Hdhbc = 2,5-dihydroxybenzoic acid and bpy = 4,4'-bipyridine), that adopted a sheet-like structure (Figure 3a).^[35] The dhbc linkers in two distinct layers are staggered, which naturally produce pores. As the π - π stacking

between the two sheets can be influenced by guest molecules, the MOF transforms to an open phase, leading to hysteretic adsorption of specific gases such as, CH₄, O₂, and N₂. The large difference in gating pressure to different gases may lead to the selective adsorption of CO₂ when controlling the partial pressure because the gating pressure of CO₂ is quite low (≈ 0.4 bar) (Figure 3b). The discoveries of MIL-53 and [Cu₂(dhbc)₂(bpy)]_n and their gas adsorption properties are regarded as pioneering discoveries in flexible MOFs. Both reports describe the gate-opening effect during adsorption, which is interesting in that although the basis for structural transformation in flexible MOFs may be different, the produced gate-opening adsorption effects are the same and can be capitalized on to enhance CO₂ separation processes.

After flexible MOFs were first studied by Kitagawa and G. Férey, the selective adsorption of CO₂ over N₂ or CH₄ inspired the field to pursue the design and synthesis of flexible MOFs for practical carbon capture. A well-studied route for the rational synthesis of

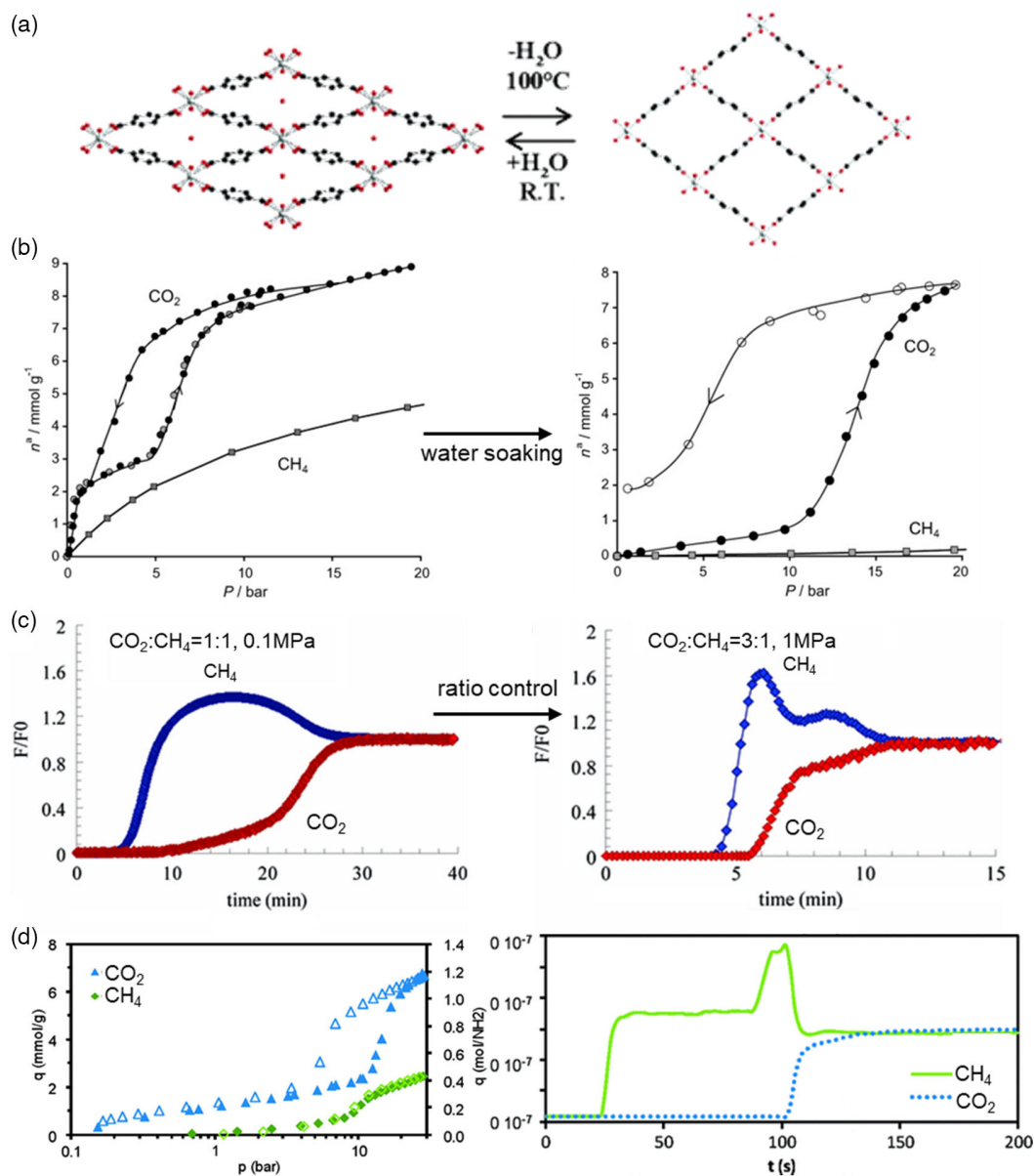


Figure 2. a) The phase transformation of MIL-53. b) The adsorption isotherms of CO₂ and CH₄ on MIL-53-Cr before and after hydration via immersing the material in water. c) The dynamic breakthrough curves for CO₂ separation on MIL-53-Cr. d) The adsorption isotherms and dynamic breakthrough curves of CO₂/CH₄ over MIL-53-Al-NH₂. a) Reproduced with permission.^[30] Copyright 2002, American Chemical Society. b) Reproduced with permission.^[32] Copyright 2006, Wiley-VCH. c) Reproduced with permission.^[33] Copyright 2009, American Chemical Society. d) Reproduced with permission.^[34] Copyright 2009, American Chemical Society.

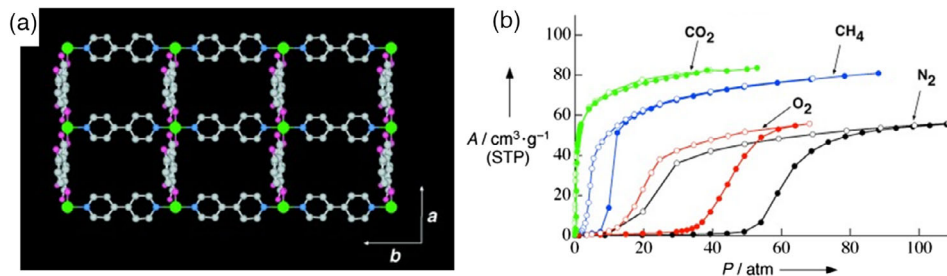


Figure 3. a) The single layer and stacking structure of [Cu₂(dhbc)₂(bpy)]_n. b) CO₂, CH₄, O₂, and N₂ adsorption performance on [Cu₂(dhbc)₂(bpy)]_n. Reproduced with permission.^[35] Copyright 2003, Wiley-VCH.

flexible MOFs is to fabricate a pillar-layer framework system. Li and co-workers reported two flexible microporous MOFs (termed MMOFs), $[\text{Zn}_2(\text{bpdc})_2(\text{bpe})]\cdot 2\text{DMF}$ (where bpdc = 4,4'-biphenyl dicarboxylate, bpe = 1,2-bis(4pyridyl)-ethane, and DMF = *N,N'*-dimethyl formamide) and $[\text{Zn}_2(\text{bpdc})_2(\text{bpee})]\cdot 2\text{DMF}$ (where bpee = 1,2-bis(4-pyridyl)ethylene), with the two organic building units serving as a “linker” and a “pillar” (Figure 4a).^[36] Interestingly from a design strategy viewpoint, the bpdc building units were observed to twist upon adsorption of polar molecules like CO_2 . This enabled these MMOFs to achieve single-component selective adsorption of CO_2 over N_2 with a separation ratio of 99:1 and 294:1 for $[\text{Zn}_2(\text{bpdc})_2(\text{bpe})]$ - and $[\text{Zn}_2(\text{bpdc})_2(\text{bpee})]$ - at a partial pressure of CO_2 of 0.16 atm, which is typical for CO_2 in the flue gas. Analysis of the exhaust after flue gas adsorption showed that the $[\text{Zn}_2(\text{bpdc})_2(\text{bpee})]\cdot 2\text{DMF}$ realized a separation ratio of 84:1 for CO_2 and N_2 at 50 °C (Figure 4b). Later, Chabal and co-workers used Raman and infrared (IR) spectroscopy to investigate the flexibility transformation of $[\text{Zn}_2(\text{bpdc})_2(\text{bpee})]\cdot 2\text{DMF}$ during CO_2 and N_2 adsorption.^[37] Combined with density functional theory (DFT) calculation, the authors suggested that upon adsorption of CO_2 , the angle between the two benzene rings of bpdc changes and the length of the C=C bond in bpee shortens, thereby producing flexibility within the overall framework (Figure 4c). Furthermore, upon simulating the adsorption site of CO_2 , the authors were able to identify the competitive interactions of the C=C bonds and C—C inter-rings with CO_2 as the reason for the rearrangement of adsorbed CO_2 molecules, all of which contribute to higher CO_2 uptake.

3. Flexibility Control for Ideal Selectivity

In practical scenarios, the CO_2 -containing gas stream is a complex, multicomponent mixture. Even if according to the

single-component adsorption isotherms of a flexible MOF, the selectivity of CO_2 over CH_4 seems to be high, structural transformation accompanied with increased pore size can lead to cooperative adsorption of CO_2 and methane. In addition, it is not easy to fit the adsorption isotherms of a flexible MOF because of gate-opening adsorption. As a result, ideal adsorbed solution theory (IAST) is not applicable for predicting separation performance; therefore, equilibrium multicomponent adsorption experiments or dynamic breakthrough experiments are important to assess the selectivity of CO_2 over CH_4 on a flexible MOF. Long and co-workers discovered that when a flexible MOF, $\text{Co}(\text{bdp})$ (where bdp = 1,4-benzenedipyrazolate), remains contracted, its pore diameter is slightly larger than the dynamic diameter of CO_2 , yet it is narrower than that of CH_4 (Figure 5a).^[38] Previously, this MOF was reported for methane storage because CH_4 can also trigger the phase transformation above a partial pressure of 15 bar.^[24] In pressure swing adsorption measurements using CO_2 and CH_4 , $\text{Co}(\text{bdp})$ adsorbed a large amount of CO_2 near 15 bar with little CH_4 uptake. The multicomponent pressure swing adsorption also revealed a reasonable selectivity of CO_2 over CH_4 , especially when carrying out the measurement with an equilibrium CO_2/CH_4 molar ratio of 6:94 (selectivity = 61 ± 4) (Figure 5b). After fitting the adsorption isotherm collected across a range of temperatures, it was suggested that the higher calculated enthalpy of adsorption for CO_2 when compared with CH_4 better satisfied the endothermic demand of $\text{Co}(\text{bdp})$.

Though the gate-opening adsorption of flexible MOFs can be capitalized in creative ways, a question persists as to how researchers can adapt flexible MOFs to the dynamic conditions (i.e., pressure, temperature, circulation, among others) found in practical applications.^[39] In this context, the precise control of flexibility appears to be difficult, but several reported attempts have suggested moving forward. A primary concern in control over flexibility is the crystal size dependence as typically

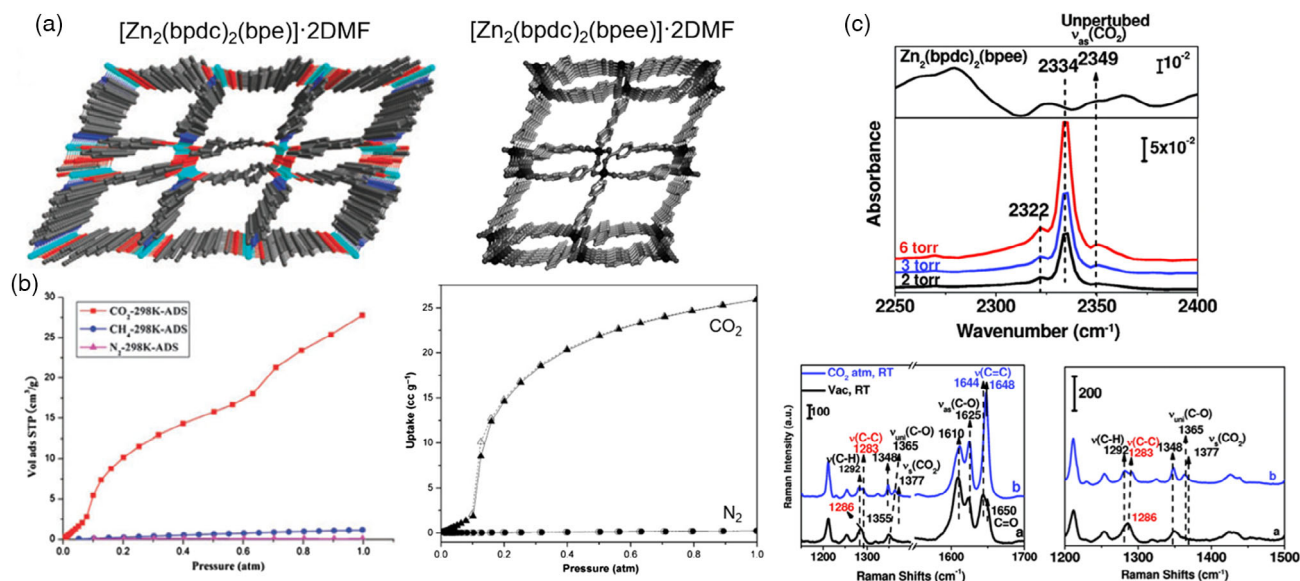


Figure 4. a) The structure of $[\text{Zn}_2(\text{bpdc})_2(\text{bpe})]\cdot 2\text{DMF}$ and $[\text{Zn}_2(\text{bpdc})_2(\text{bpee})]\cdot 2\text{DMF}$. b) CO_2 and N_2/CH_4 adsorption isotherms of the two MMOFs. c) The IR and Raman spectra for $[\text{Zn}_2(\text{bpdc})_2(\text{bpee})]\cdot 2\text{DMF}$ in the presence and absence of CO_2 . a, b) left: Reproduced with permission.^[36a] Copyright 2010, Royal Society of Chemistry. right: Reproduced with permission.^[36b] Copyright 2010, Wiley-VCH. c) Reproduced with permission.^[37] Copyright 2011, American Chemical Society.

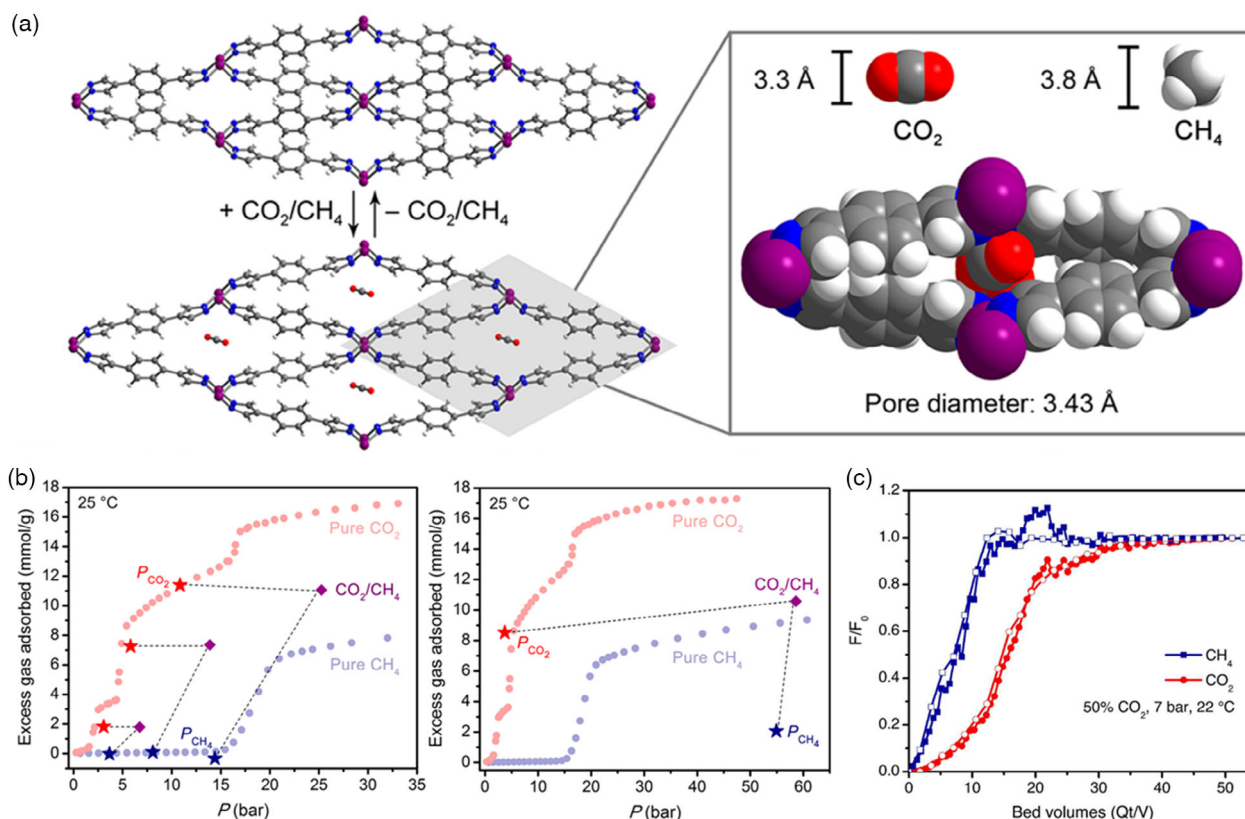


Figure 5. a) Front view of Co(bdp) before and after adsorbing CO₂. b) Multicomponent pressure swing adsorption of CO₂ and CH₄ on Co(bdp). c) Breakthrough curves of CO₂ and CH₄ with different flow rates (open symbol: 15 sccm; filled symbol: 5 sccm) over Co(bdp). Reproduced with permission.^[38] Copyright 2018, American Chemical Society.

MOFs with uniform and large crystal sizes have better cooperativity. Specifically, the crystal size of a given flexible MOF can influence the gate-opening pressure, and in extreme crystal size conditions, these MOFs may undergo a shape memory effect or in other words, lose flexibility.

Kitagawa and co-workers modulated the crystal size of a twofold interpenetrated flexible MOF [Cu₂(bdc)₂(bpy)]_n.^[40] Acetic acid was initially added and reacted with copper (II) ions. This was followed by reacting a mixture of the newly formed copper acetate with H₂bdc and bpy, so that the crystal size is controlled at a submicrometer stage. The crystal size was observed to change with the concentration ratio of acetic acid and the resulting adsorption isotherms gradually changed with the crystal size. This proved that the barrier of transformation in a given flexible MOF is caused by kinetic suppression with large crystal size being more difficult to overcome (Figure 6). In situ PXRD measurements coupled to methanol adsorption isotherms indicated that the crystal structure of mesosize retains an open phase after the desorption of methanol and does not transform. It is only when the crystal is heated to over 200 °C that the MOF transforms to the contraction phase, yet the structure reversibly recovers its open phase after adsorption. Similar dynamic structural flexibility was also observed for [Cu₂(bdc)₂(bpy)]_n during CO₂ adsorption. In the context of CO₂ separation, the gating adsorption effect is quite essential because it can define the working capacity for carbon capture.

Crystal size-dependent flexibility is not necessarily a peculiar phenomenon. From 2010 to 2012, Kaskel, Brunner, and co-workers reported a series of MOFs termed the DUT-8 series (M₂(2,6-ndc)₂(dabco), where 2,6-ndc = 2,6-naphthalenedicarboxylate and dabco = 1,4-diazabicyclo[2.2.2]octane).^[41] The flexibility of DUT-8-Ni and DUT-8-Co was proven through ¹²⁹Xe nuclear magnetic resonance (NMR) spectroscopy measurements alongside PXRD analysis. The selective high-pressure adsorption of CO₂ versus CH₄, N₂, and O₂ on DUT-8-Ni provides further indication of the gate-opening adsorption behavior of the framework. Kaskel, Bon, and co-workers altered the synthesis conditions to prepare DUT-8-Ni with submicrometer crystal size and measured the N₂ adsorption isotherms for different crystal sizes (Figure 7a).^[42] The N₂ adsorption performance indicates that for crystals of DUT-8-Ni with a size below 500 nm, the structure remains rigid in the expanded phase after solvent removal with no observed gating adsorption (Figure 7b). Electron paramagnetic resonance (EPR) and IR spectroscopies confirmed a large concentration of defects in smaller crystals of DUT-8-Ni, which may be the reason for the observed structural rigidity.

It is noted that the interaction between a given framework and CO₂ can sometimes not be strong enough to drive the expansion of a flexible framework and, in these cases, it may be necessary to regulate the transformation in alternative ways. A representative example is that of (Me₂NH₂)[In(ABDC)₂] (where

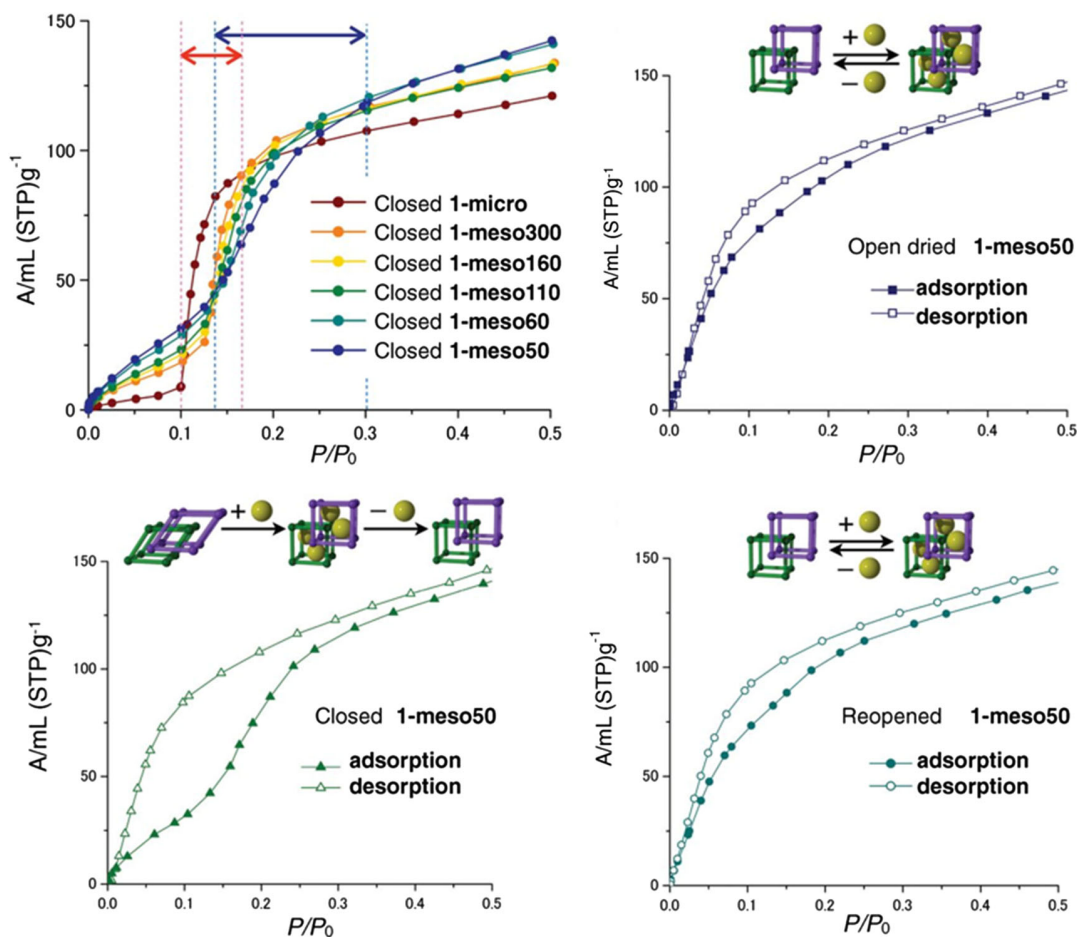


Figure 6. Different adsorption performances of methanol on different $[\text{Cu}_2(\text{bdc})_2(\text{bpy})]_n$ crystal sizes when solvent soaked, dried, and reopened. Reproduced with permission.^[40] Copyright 2013, The American Association for the Advancement of Science.

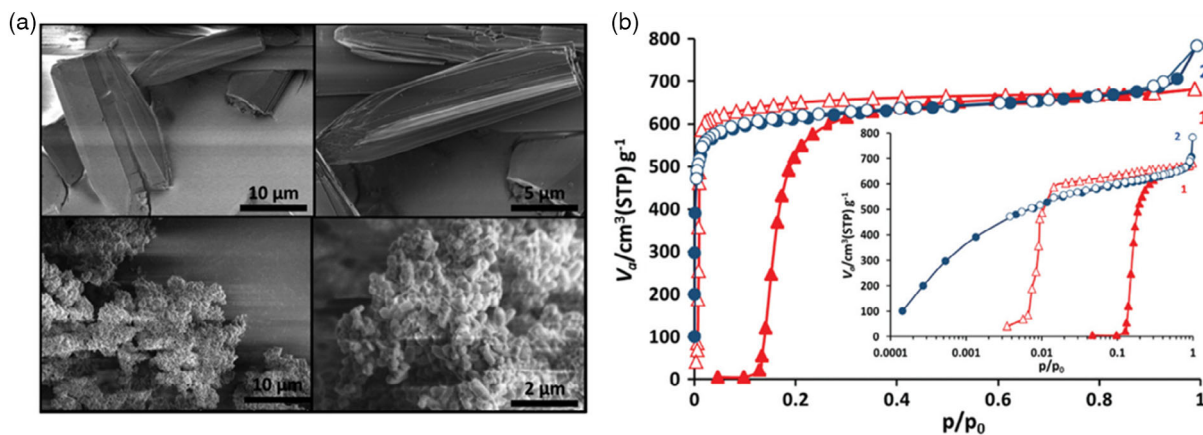


Figure 7. a) SEM image demonstrating the crystal size between flexible (up) and rigid (bottom) DUT-8-Ni. b) Different adsorption performances of flexible (1) and rigid (2) DUT-8-Ni. Reproduced with permission.^[42a] Copyright 2017, Royal Society of Chemistry.

ABDC = 2-aminobenzene-1,4-dicarboxylate), also known as SHF-61.^[43] SHF-61 achieves a porous structure after the removal of different solvent molecules. Brammer and co-workers reported that for solvent molecules like DMF, the framework

can exhibit continuous-breathing behavior during activation with the MOF ultimately settling into a contracted phase (**Figure 8a**). However, for solvent molecules such as CHCl_3 , SHF-61 retains its expanded phase even after desolvation. Furthermore, when

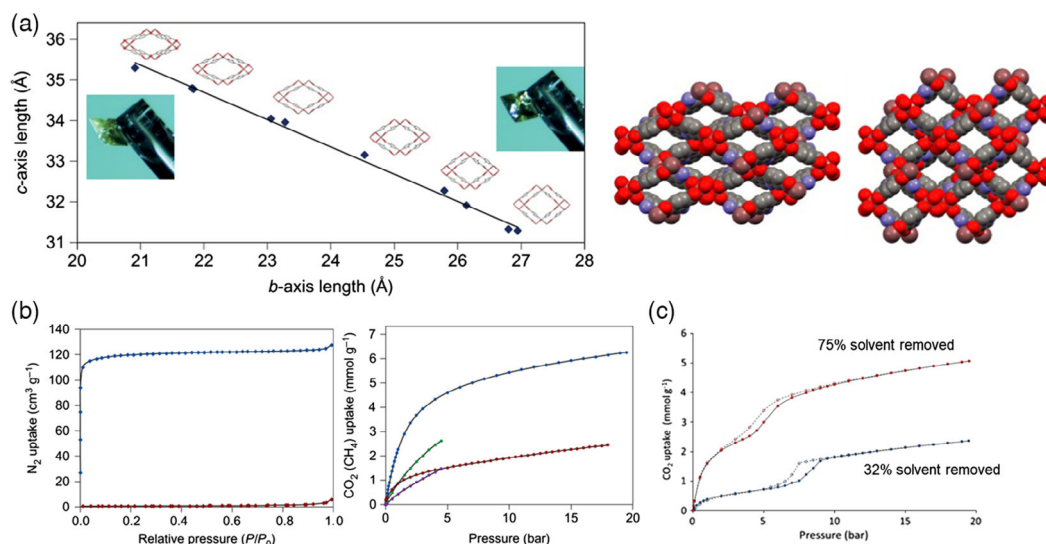


Figure 8. a) Continuous-breathing behavior of SHF-61-DMF. b) Adsorption behavior of N₂, CO₂, and CH₄ on SHF-61. c) Gate-opening adsorption of CO₂ on SHF-61-DMF with 32% and 75% solvent removed. Reproduced with permission.^[43] Copyright 2017, Springer Nature.

the framework is in its contracted phase, CO₂ cannot produce the breathing effect even at high pressures, so the uptake of CO₂ remains as low as CH₄ or even lower over 5 bars of pressure (Figure 8b). It is only when a few DMF molecules are remaining within the framework that CO₂ can trigger structural transformation to the expanded phase. In situ PXRD measurement revealed SHF-61's different responses to CO₂ and CH₄ when DMF is present within the framework. Accordingly, when SHF-61 was partially activated, distinct selective adsorption between CO₂ and CH₄ was performed (Figure 8c,d).

4. Practical Challenges and Potential Solutions

It follows that if there is gate-opening adsorption over a suitable pressure range, flexible MOFs have a high potential for use in the carbon capture process. However, in practical scenarios, especially at high pressure, challenges still pose in process engineering that can impact flexible MOF performance beyond pure chemistry.

One such challenge is the crushing of MOF crystals. This problem was identified in 2013, when Farha, Yildirim, and co-workers attempted to increase the packing density of HKUST-1 ([Cu₃(TMA)₂(H₂O)₃]_n, where TMA = trimesic acid), in which they found that upon physically crushing the MOF crystals, the working capacity for methane storage was impaired.^[44] Especially for flexible MOFs, there can be another trigger besides high working pressure, which is that as the structural transformation occurs, the cell volume usually changes, and the expansion–shrinkage process will sometimes lead to crystals being crushed even if the pressure of the adsorption–desorption cycles is low. This finding points to a potential problem faced by flexible MOFs in that, if a given MOF crystal is crushed, then the flexibility of the structure may also be lost even if porosity is retained. When the crystal size approaches the mesosize scale, the gate opening adsorption performance disappears and the superior properties of flexible MOFs become unstable over the course of multiple-

cycle use. Kaskel and co-workers observed crushing of a flexible MOF, DUT-98 (Zr₆O₄(OH)₄(CPCDC)₄(H₂O)₄, where CPCDC = 9-(4-carboxyphenyl)-9H-carbazole-3,6-dicarboxylate) after adsorption experiments of N₂ (at 77 K), CO₂ (at 195 K), *n*-butane (at 273 K), and various alcohols (at 298 K) (Figure 9a).^[45] Although the pressure was not high, significant differences were observed between the adsorption isotherms and the scanning electron microscope (SEM) images, indicating a close relationship between the adsorption performance change and the crushing of DUT-98's crystals (Figure 9b,c). To solve the problem of crushing, a reasonable route to pursue is the pelletization of flexible MOFs as pellets can partly resist the pressure and the flexible behavior will remain. Zhao and co-workers compacted flexible MOFs, MIL-53(Al)-OH and MIL-53(Al)-(OH)₂, into 8.5 mm pellets and demonstrated that the adsorption isotherms with gate-opening effects were maintained (Figure 9d,e).^[46] Unfortunately, the pellets were crushed after high-pressure CH₄ adsorption experiments. A better way to use flexible MOFs is to construct them through stronger chemical bonds as the crushing of these MOF crystals is usually accompanied with the breaking of their bonds. Covalent organic frameworks (COFs) are constructed by organic linkers exclusively through covalent bonds,^[47] and there have been several reports of these materials having flexibility and gate-opening adsorption behavior.^[48] The application of flexible COFs in carbon capture in the future is extremely attractive because of the high bond energy of noncoordinative covalent bonds.

Another challenge is that of slipping-off. When performing dynamic breakthrough experiments, the outlet gas contains a small concentration of CO₂ initially because the uptake of CO₂ on flexible MOFs below the partial pressure of the gate-opening effect is quite poor. This means that the flexible MOF cannot complete separation under low CO₂ partial pressure and gas-flowing conditions. At higher total pressure conditions, the uptake of CO₂ at low partial pressure cannot cover the amount of CO₂ in a given gas mixture usually. An example is

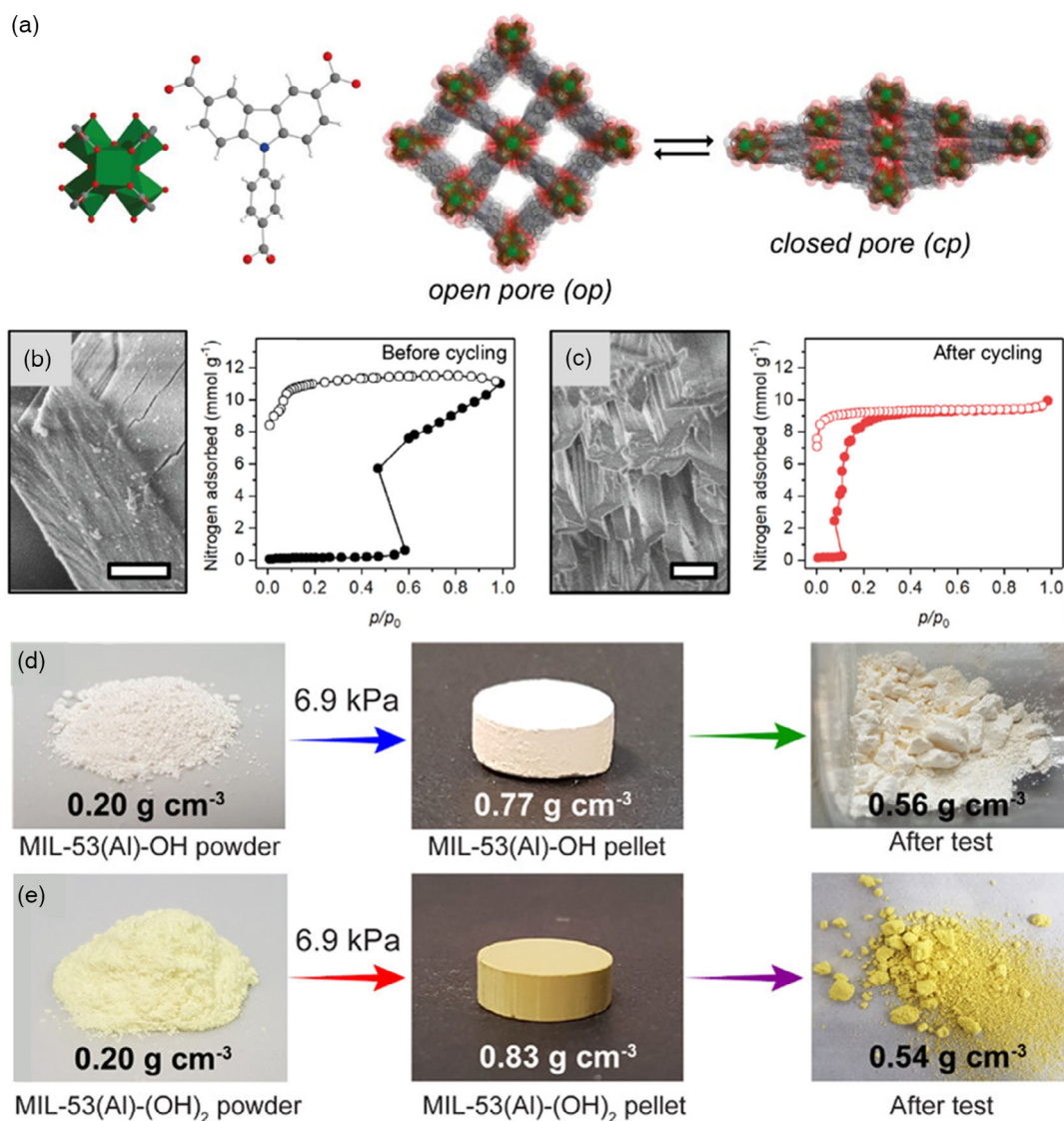


Figure 9. a) Secondary building unit, organic linker, and phase change of DUT-98. b,c) SEM image and adsorption isotherm of DUT-98 before (b) and after (c) the cycling adsorption experiment. d,e) The character of MIL-53(Al)-OH (d) and MIL-53(Al)-(OH)₂ (e) under the condition of powder, pellet, and after the test. a) Reproduced with permission.^[45a] Copyright 2019, Wiley-VCH. b,c) Reproduced under terms of the CC-BY license.^[45b] Copyright 2019, The Authors. Published by Beilstein-Institut. d,e) Reproduced with permission.^[46] Copyright 2019, American Chemical Society.

Co(bdp), in which the authors reported the dynamic breakthrough measurement with CO₂ and CH₄ being detected at the outlet at the same time, indicating that there is no effective separation (Figure 5c).^[38] Indeed, this was different from the result of multicomponent adsorption. A different work reported by Sotomayor and Lastoskie proved that this slipping-off phenomenon also exists in ELM-11 (Figure 10a).^[49] According to the work developed by Miyahara, Tanaka, and co-workers,^[50] ELM-11 was used for the separation of CO₂/CH₄ with the gate response to CO₂ occurring around 50 kPa with a different MOF, HKUST-1, being introduced to address the slipping-off (Figure 10b). Even though the selectivity of CO₂/CH₄ on HKUST-1 (8.67) is not as high as ELM-11 (82.3), HKUST-1 possesses a decent CO₂ uptake below a partial pressure of 50 kPa, which successfully overcomes ELM-11's slipping-off

(Figure 10c). The two-MOF system can produce pure CH₄ from a mixture of CO₂/CH₄ with the majority of CO₂ (over 80%) being captured by ELM-11, which reflects the high working capacity of flexible MOFs.

A final challenge is the machine shaping of flexible MOFs. Because the cell volume may shrink and expand with changes to a given flexible MOF's structure, the volume of single crystals may alter in a range when shaping, which causes difficulties to film building and fabrication in confined space. Flexible binders are thought to help with the shaping of flexible MOFs with their flexibility being maintained. Hartmann and co-workers reported a facile and effective approach to shape MIL-53(Al) (Figure 11a).^[51] They used methyl cellulose (MC 400 and MC 4000) as organic binders to shape MIL-53(Al) to extrudates. PXRD experiments and N₂ adsorption isotherms at 77 K

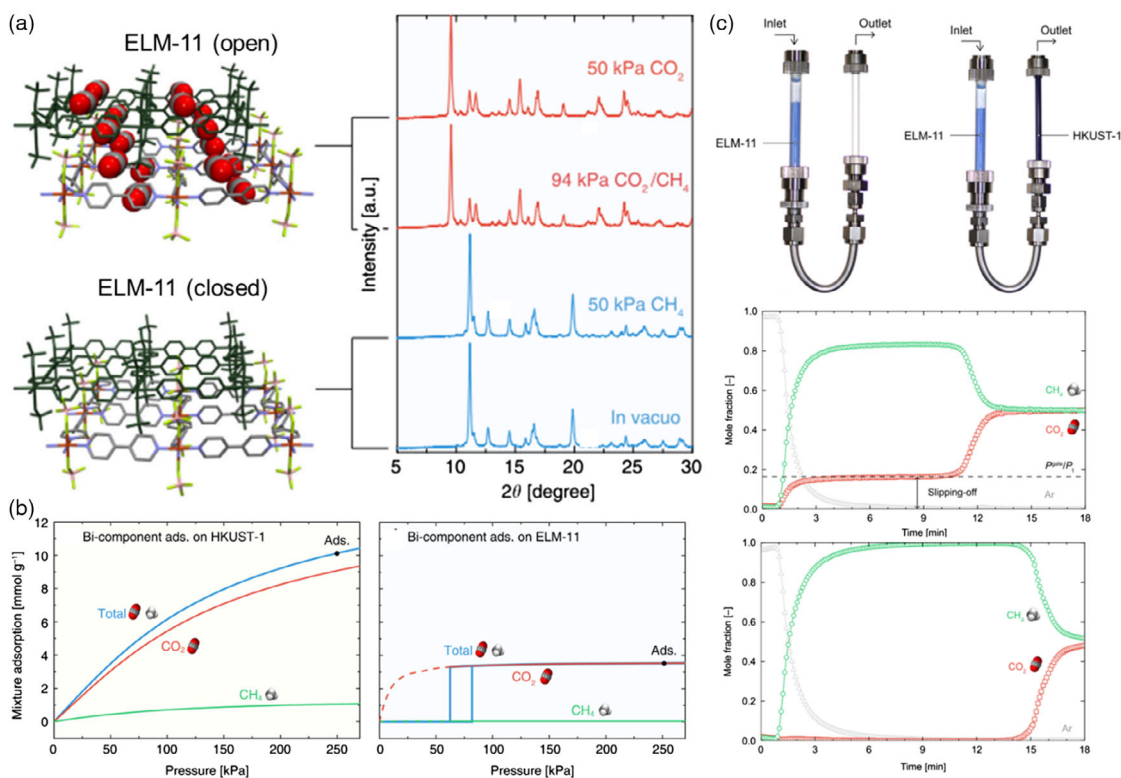


Figure 10. a) Open and closed phases of the crystal structure of ELM-11. b) CO_2/CH_4 component adsorption performance between HKUST-1 and ELM-11. c) Dynamic breakthrough curves before and after combining ELM-11 with HKUST-1 in a breakthrough bed. Reproduced under terms of the CC-BY license.^[50] Copyright 2020, The Authors. Published by Springer Nature.

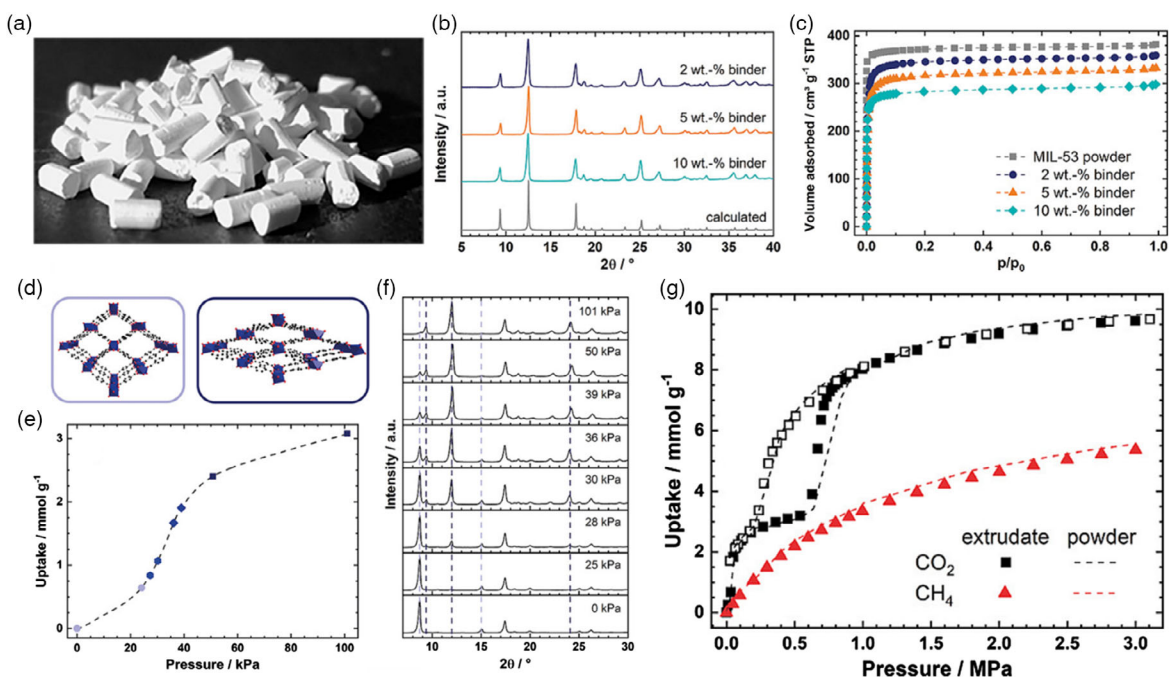


Figure 11. a) Photograph of fabricated MIL-53(Al) extrudates. b) PXRD patterns of MIL-53(Al) extrudates with different amounts of MC 400. c) Nitrogen adsorption isotherms at 77 K of the MIL-53(Al) extrudates in comparison with the parent powder. d) Structural view of MIL-53(p) (left) and MIL-53np (right). e) CO_2 adsorption isotherm of MIL-53(Al) extrudates at 30 °C. f) In situ PXRD patterns of MIL-53(Al) extrudates corresponding to CO_2 adsorption. g) High-pressure methane and carbon dioxide adsorption isotherms at 30 °C on MIL-53(Al) MC 4000 3 wt% of binder in comparison with the adsorption isotherms on MIL-53(Al) powder. Reproduced under terms of the CC-BY license.^[51] Copyright 2019, The Authors. Published by Wiley-VCH.

indicated that crystallinity and porosity were retained after shaping (Figure 11b,c). A small relative reduction of 1.5–10.6% prevails over extrudates with different organic binders reported before. The following in situ PXRD experiment corresponding to CO₂ adsorption (Figure 11e,f) and high-pressure CO₂ and CH₄ adsorption isotherms (Figure 11g) proved that the shaped MIL-53(Al) retains its ability to undergo structural transformation and gate-opening adsorption. The enhancement of mechanical and chemical stability of the extrudates is proven by vertical crushing stress tests and immersion in organic solvents. When 5 wt% of MC 4000 is used, the probability of failure of the extrudates is below 10%. Furthermore, the extrudates are stable in *n*-heptane for more than 9 months. Amino-functionalized MIL-53(Al) was also shaped in a similar manner and the flexibility was retained as well. Another solution for shaping flexible MOFs is to rely on rational synthesis to produce flexible MOFs that only change the pore aperture feature instead of cell volume when gate-opening adsorption occurs. Indeed, new and improved methods to address this challenge are needed.

Received: November 23, 2021

Revised: January 17, 2022

Published online:

5. Outlook

Flexible MOFs have great potential for energy-efficient carbon capture because of their greater working capacity, ideal adsorption selectivity, and intrinsic thermal management. Molecular understanding of the adsorption mechanisms plays an important role in further propelling flexible MOFs into practical applications. Advanced characterizations, such as in situ gas adsorption crystallography and spectroscopy, in conjunction with molecular simulation, are useful for uncovering adsorptive sites, host–guest interaction, guest–guest arrangement, and the energy barrier for structural transformation.^[52] Material discovery powered by artificial intelligence is a powerful tool in the large-scale screening of desired MOFs with superior performance^[53] and when coupled with automated high-throughput experiments, is favorable for accelerating the synthesis of targeted flexible MOFs.^[54]

Acknowledgements

The authors acknowledge financial support from the National Natural Science Foundation of China (nos. 21522105 and 51861145313), the Science and Technology Commission of Shanghai Municipality (nos. 21XD1402300, 21JC1401700, and 21DZ2260400), the Alliance of International Science Organization (ANSO-CR-PP-2020-06), and the Research Startup Fund of ShanghaiTech University. K.E.C is grateful for the support provided by the Jordan Ministry of Higher Education and Scientific Research (project no. BAS/1/6/202).

Conflict of Interest

The authors declare no conflict of interest.

Keywords

carbon capture, flexible metal–organic frameworks, intrinsic thermal management, selectivities, working capacities

- [1] R. F. Keeling, C. D. Keeling, *Atmospheric Monthly In Situ CO₂ Data-Mauna Loa Observatory, Hawaii, In Scripps CO₂ Program Data*. UC San Diego Library Digital Collections, **2017**, <https://doi.org/10.6075/J08W3BHW> (accessed: November 2021).
- [2] *World Meteorological Organization, WMO Statement on the State of the Global Climate in 2016*. <https://public.wmo.int/en/resources/library/wmo-statement-state-of-global-climate-2016> (accessed: November 2021).
- [3] M. Kennedy, D. Mrofka, C. von der Borch, *Nature* **2008**, *453*, 642.
- [4] G. A. Ozin, M. F. Ghossoub, *The Story of CO₂: Big Ideas for a Small Molecule*, University of Toronto Press, Toronto, Canada **2020**.
- [5] Masson-Delmotte, V., P. Zhai, H.-O. Pörtner, D. Roberts, J. Skea, P. R. Shukla, A. Pirani, W. Moufouma-Okia, C. Péan, R. Pidcock, S. Connors, J. B. R. Matthews, Y. Chen, X. Zhou, M. I. Gomis, E. Lonnoy, T. Maycock, M. Tignor, T. Waterfield, *Global Warming of 1.5°C*, <https://www.ipcc.ch/sr15/> (accessed: November 2021).
- [6] a) G. T. Rochelle, *Science* **2009**, *325*, 1652; b) D. W. Keith, G. Holmes, D. St. Angelo, K. Heidel, *Joule* **2018**, *2*, 1573.
- [7] A. Zhao, A. Samanta, P. Sarkar, R. Gupta, *Ind. Eng. Chem. Res.* **2013**, *52*, 6480.
- [8] A. Kumar, D. G. Madden, M. Lusi, K.-J. Chen, E. A. Daniels, T. Curtin, J. J. Perry IV, M. J. Zaworotko, *Angew. Chem., Int. Ed.* **2015**, *54*, 14372.
- [9] R. L. Siegelman, E. J. Kim, J. R. Long, *Nat. Mater.* **2021**, *20*, 1060.
- [10] a) R. V. Siriwardane, M. S. Shen, E. P. Fisher, J. A. Poston, *Energy Fuels* **2001**, *15*, 279; b) F. Su, C. Lu, *Energy Environ. Sci.* **2012**, *5*, 9021; c) Y. Zhou, J. Zhang, L. Wang, X. Cui, X. Liu, S. S. Wong, H. An, N. Yan, J. Xie, C. Yu, P. Zhang, Y. Du, S. Xi, L. Zheng, X. Cao, Y. Wu, Y. Wang, C. Wang, H. Wen, L. Chen, H. Xing, J. Wang, *Science* **2021**, *373*, 315.
- [11] a) T. A. Makal, J.-R. Li, W. Lu, H.-C. Zhou, *Chem. Soc. Rev.* **2012**, *41*, 7761; b) Y. He, W. Zhou, G. Qian, B. Chen, *Chem. Soc. Rev.* **2014**, *43*, 5657; c) O. M. Yaghi, M. J. Kalmutzki, C. S. Diercks, *Introduction to Reticular Chemistry: Metal-Organic Frameworks and Covalent Organic Frameworks*, Wiley-VCH, Weinheim **2019**.
- [12] a) W. R. Lee, H. Jo, L.-M. Yang, H. Lee, D. W. Ryu, K. S. Lim, J. H. Song, D. Y. Min, S. S. Han, J. G. Seo, Y. K. Park, D. Moon, C. S. Hong, *Chem. Sci.* **2015**, *6*, 3697; b) N. T. T. Nguyen, H. Furukawa, F. Gandara, H. T. Nguyen, K. E. Cordova, O. M. Yaghi, *Angew. Chem., Int. Ed.* **2014**, *53*, 10645; c) Z. Shi, Y. Tao, J. Wu, C. Zhang, H. He, L. Long, Y. Lee, T. Li, Y.-B. Zhang, *J. Am. Chem. Soc.* **2020**, *142*, 2750; d) O. T. Qazvini, S. G. Telfer, *ACS Appl. Mater. Interfaces* **2021**, *13*, 12141; e) J. M. Kolle, M. Fayaz, A. Sayari, *Chem. Rev.* **2021**, *121*, 7280.
- [13] a) J. M. Simmons, H. Wu, W. Zhou, T. Yildirim, *Energy Environ. Sci.* **2011**, *4*, 2177; b) K. Sumida, D. L. Rogow, J. A. Mason, T. M. McDonald, E. D. Bloch, Z. R. Herm, T.-H. Bae, J. R. Long, *Chem. Rev.* **2012**, *112*, 724. c) C. A. Trickett, A. Helal, B. A. Al-Maythaly, Z. H. Yamani, K. E. Cordova, O. M. Yaghi, *Nat. Rev. Mater.* **2017**, *2*, 17045.
- [14] a) M. Ding, R. W. Flaig, H.-L. Jiang, O. M. Yaghi, *Chem. Soc. Rev.* **2019**, *48*, 2783; b) W. D. Jones, *J. Am. Chem. Soc.* **2020**, *142*, 4955. c) C. S. Diercks, Y. Liu, K. E. Cordova, O. M. Yaghi, *Nat. Mater.* **2018**, *17*, 301.
- [15] S. J. Datta, C. Khumnoon, Z. H. Lee, W. K. Moon, S. Docao, T. H. Nguyen, I. C. Hwang, D. Moon, P. Oleynikov, O. Terasaki, K. B. Yoon, *Science* **2015**, *350*, 302.
- [16] a) P. Nugent, Y. Belmabkhout, S. D. Burd, A. J. Cairns, R. Luebke, K. Forrest, T. Pham, S. Ma, B. Space, L. Wojtas, M. Eddaoudi,

- M. J. Zaworotko, *Nature* **2013**, *495*, 80; b) O. Shekhah, Y. Belmabkhout, Z. Chen, V. Guillerm, A. Cairns, K. Adil, M. Eddaoudi, *Nat. Commun.* **2014**, *5*, 4228; c) S. Mukherjee, N. Sikdar, D. O'Nolan, D. M. Fran, V. Gascón, A. Kumar, N. Kumar, H. S. Scott, D. G. Madden, P. E. Kruger, B. Space, M. J. Zaworotko, *Sci. Adv.* **2019**, *5*, 9171.
- [17] a) L.-J. Li, P.-Q. Liao, C.-T. He, Y.-S. Wei, H.-L. Zhou, J.-M. Lin, X.-Y. Li, J.-P. Zhang, *J. Mater. Chem. A* **2015**, *3*, 21849; b) Q. Yang, S. Vaesen, F. Ragon, A. D. Wiersum, D. Wu, A. Lago, T. Devic, C. Martineau, F. Taulelle, P. L. Llewellyn, H. Jobic, C. Zhong, C. Serre, G. De Weireld, G. Maurin, *Angew. Chem., Int. Ed.* **2013**, *52*, 10316.
- [18] a) S. R. Caskey, A. G. Wong-Foy, A. J. Matzger, *J. Am. Chem. Soc.* **2008**, *130*, 10870; b) B. Li, Z. Zhang, Y. Li, K. Yao, Y. Zhu, Z. Deng, F. Yang, X. Zhou, G. Li, H. Wu, N. Nijem, Y. J. Chabal, Z. Lai, Y. Han, Z. Shi, S. Feng, J. Li, *Angew. Chem., Int. Ed.* **2012**, *51*, 1412.
- [19] H. Zeng, M. Xie, T. Wang, R.-J. Wei, X.-J. Xie, Y. Zhao, W. Lu, D. Li, *Nature* **2021**, 595, 542.
- [20] a) S. Horike, S. Shimomura, S. Kitagawa, *Nat. Chem.* **2009**, *1*, 695; b) A. Schneemann, V. Bon, I. Schwedler, I. Senkovska, S. Kaskel, R. A. Fischer, *Chem. Soc. Rev.* **2014**, *43*, 6062; c) S. K. Elsaidi, M. H. Mohamed, D. Banerjee, P. K. Thallapally, *Coord. Chem. Rev.* **2018**, *358*, 125.
- [21] P. L. Llewellyn, G. Maurin, T. Devic, S. Loera-Serna, N. Rosenbach, C. Serre, S. Bourrelly, P. Horcajada, Y. Filinchuk, G. Férey, *J. Am. Chem. Soc.* **2008**, *130*, 12808.
- [22] a) C. Serre, F. Millange, S. Surblé, G. Férey, *Angew. Chem., Int. Ed.* **2004**, *43*, 6285; b) C. Serre, C. Mellot-Draznieks, S. Surblé, N. Audebrand, Y. Filinchuk, G. Férey, *Science* **2007**, *315*, 1828.
- [23] S. Yang, X. Lin, W. Lewis, M. Suyetin, E. Bichoutskaia, J. E. Parker, C. C. Tang, D. R. Allan, P. J. Rizkallah, P. Hubberstey, N. R. Champness, K. M. Thomas, A. J. Blake, M. Schröder, *Nat. Mater.* **2012**, *527*, 357.
- [24] J. A. Mason, J. Oktawiec, M. K. Taylor, M. R. Hudson, J. Rodriguez, J. E. Bachman, M. I. Gonzalez, A. Cervellino, A. Guagliardi, C. M. Brown, P. L. Llewellyn, N. Masciocchi, J. R. Long, *Nature* **2015**, *527*, 357.
- [25] D. Li, K. Kaneko, *Chem. Phys. Lett.* **2001**, *335*, 50.
- [26] A. Kondo, H. Noguchi, S. Ohnishi, H. Kajiro, A. Tohdoh, Y. Hattori, W.-C. Xu, H. Tanaka, H. Kanoh, K. Kaneko, *Nano Lett.* **2006**, *6*, 2581.
- [27] Y. Cheng, H. Kajiro, H. Noguchi, A. Kondo, T. Ohba, Y. Hattori, K. Kaneko, H. Kanoh, *Langmuir* **2011**, *27*, 6905.
- [28] V. Bon, I. Senkovska, D. Wallacher, A. Heerwig, N. Klein, I. Zizak, R. Feyerherm, E. Dudzik, S. Kaskel, *Microporous Mesoporous Mater.* **2014**, *188*, 190.
- [29] M. Ichikawa, A. Kondo, H. Noguchi, N. Kojima, T. Ohba, H. Kajiro, Y. Hattori, H. Kanoh, *Langmuir* **2016**, *32*, 9722.
- [30] C. Serre, F. Millange, C. Thouvenot, M. Noguès, G. Marsolier, D. Louër, G. Férey, *J. Am. Chem. Soc.* **2002**, *124*, 13519.
- [31] S. Bourrelly, P. L. Llewellyn, C. Serre, F. Millange, T. Loiseau, G. Férey, *J. Am. Chem. Soc.* **2005**, *127*, 13519.
- [32] P. L. Llewellyn, S. Bourrelly, C. Serre, Y. Filinchuk, G. Férey, *Angew. Chem., Int. Ed.* **2006**, *45*, 7751.
- [33] L. Hamon, P. L. Llewellyn, T. Devic, A. Ghoufi, G. Clet, V. Guillerm, G. D. Pirngruber, G. Maurin, C. Serre, G. Driver, W. van Beek, E. Jolimaître, A. Vimont, M. Daturi, G. Férey, *J. Am. Chem. Soc.* **2009**, *131*, 17490.
- [34] S. Couck, J. F. M. Denayer, G. V. Baron, T. Rémy, J. Gascon, F. Kapteijn, *J. Am. Chem. Soc.* **2009**, *131*, 6326.
- [35] R. Kitaura, K. Seki, G. Akiyama, S. Kitagawa, *Angew. Chem., Int. Ed.* **2003**, *42*, 428.
- [36] a) J. Zhang, H. Wu, T. J. Emgea, J. Li, *Chem. Commun.* **2010**, *46*, 9152; b) H. Wu, R. S. Reali, D. A. Smith, M. C. Trachtenberg, J. Li, *Chem.-Eur. J.* **2010**, *16*, 13951.
- [37] N. Nijem, P. Thissen, Y. Yao, R. C. Longo, K. Roodenko, H. Wu, Y. Zhao, K. Cho, J. Li, D. C. Langreth, Y. J. Chabal, *J. Am. Chem. Soc.* **2011**, *133*, 12849.
- [38] M. K. Taylo, T. Runčevski, J. Oktawiec, J. E. Bachman, R. L. Siegelman, H. Jiang, J. A. Mason, J. D. Tarver, J. R. Long, *J. Am. Chem. Soc.* **2018**, *140*, 10324.
- [39] J.-P. Zhang, H.-L. Zhou, D.-D. Zhou, P.-Q. Liao, X.-M. Chen, *Natl. Sci. Rev.* **2018**, *5*, 907.
- [40] Y. Sakata, S. Furukawa, M. Kondo, K. Hirai, N. Horike, Y. Takashima, H. Uehara, N. Louvain, M. Meilikhov, T. Tsuruoka, S. Isoda, W. Kosaka, O. Sakata, S. Kitagawa, *Science* **2013**, *339*, 193.
- [41] a) N. Klein, C. Herzog, M. Sabo, I. Senkovska, J. Getzschmann, S. Paasch, M. R. Lohe, E. Brunner, S. Kaskel, *Phys. Chem. Chem. Phys.* **2010**, *12*, 11778; b) N. Klein, H. C. Hoffmann, A. Cadiou, J. Getzschmann, M. R. Lohe, S. Paasch, T. Heydenreich, K. Adil, I. Senkovska, E. Brunner, S. Kaskel, *J. Mater. Chem.* **2012**, *22*, 10303.
- [42] a) N. Kavooosi, V. Bon, I. Senkovska, S. Krause, C. Atzori, F. Bonino, J. Pallmann, S. Paasch, E. Brunner, S. Kaskel, *Dalton Trans.* **2017**, *46*, 4685; b) H. Miura, V. Bon, I. Senkovska, S. Ehrling, S. Watanabe, M. Ohbam, S. Kaskel, *Dalton Trans.* **2017**, *46*, 14002.
- [43] E. J. Carrington, C. A. McAnally, A. J. Fletcher, S. P. Thompson, M. Warren, L. Brammer, *Nat. Chem.* **2019**, *9*, 882.
- [44] Y. Peng, V. Krungleviciute, I. Eryazici, J. T. Hupp, O. K. Farha, T. Yildirim, *J. Am. Chem. Soc.* **2013**, *135*, 11887.
- [45] a) S. Krause, V. Bon, U. Stoeck, I. Senkovska, D. M. Többsen, D. Wallacher, S. Kaskel, *Angew. Chem., Int. Ed.* **2017**, *56*, 10676; b) S. Krause, V. Bon, H. Du, R. E. Dunin-Borkowski, U. Stoeck, I. Senkovska, S. Kaskel, *Beilstein J. Nanotechnol.* **2019**, *10*, 1737.
- [46] T. Kundu, B. B. Shah, L. Bolinois, D. Zhao, *Chem. Mater.* **2019**, *31*, 2842.
- [47] a) C. S. Diercks, O. M. Yaghi, *Science*, **2017**, *355*, 293; b) S. J. Lyle, P. J. Waller, O. M. Yaghi, *Trends Chem.* **2019**, *1*, 172.
- [48] a) Y.-B. Zhang, J. Su, H. Furukawa, Y. Yun, F. Gándara, A. Duong, X. Zou, O. M. Yaghi, *J. Am. Chem. Soc.* **2013**, *135*, 16336; b) Y. X. Ma, Z. J. Li, L. Wei, S. Y. Ding, Y.-B. Zhang, W. Wang, *J. Am. Chem. Soc.* **2017**, *139*, 4995; c) Y. Chen, Z.-L. Shi, L. Wei, B. Zhou, J. Tan, H.-L. Zhou, Y.-B. Zhang, *J. Am. Chem. Soc.* **2019**, *141*, 3298.
- [49] F. J. Sotomayor, C. M. Lastoskie, *Langmuir* **2017**, *33*, 11670.
- [50] S. Hiraide, Y. Sakanaka, H. Kajiro, S. Kawaguchi, M. T. Miyahara, H. Tanaka, *Nat. Commun.* **2020**, *11*, 3867.
- [51] M. Kriesten, J. V. Schmitz, J. Siegel, C. E. Smith, M. Kaspereit, M. Hartmann, *Eur. J. Inorg. Chem.* **2019**, *43*, 4700.
- [52] a) V. Bon, E. Brunner, A. Poppl, S. Kaskel, *Adv. Fun. Mater.* **2020**, *30*, 1907847. b) J. Yu, L.-H. Xie, J.-R. Li, Y. Ma, J. M. Seminario, P. B. Balbuena, *Chem. Rev.* **2017**, *117*, 9674.
- [53] a) P. G. Boyd, A. Chidambaram, E. García-Díez, C. P. Ireland, T. D. Daff, R. Bounds, A. Gładysiak, P. Schouwink, S. M. Moosavi, M. M. Maroto-Valer, J. A. Reimer, J. A. R. Navarro, T. K. Woo, S. Garcia, K. C. Stylianou, B. Smit, *Nature* **2019**, *576*, 253; b) X. Zhang, K. Zhang, Y. Lee, *ACS Appl. Mater. Interfaces* **2020**, *12*, 734.
- [54] H. Reinsch, N. Stock, *Microporous Mesoporous Mater.* **2013**, *171*, 156.



Xuan Yao obtained his B.Sc. degree from Shanghai Jiao Tong University in 2019. He is now a Ph.D. candidate at the School of Physical Science and Technology, ShanghaiTech University. His research interest is the crystallochemistry and structure–activity relationships of dynamic covalent organic frameworks.



Kyle E. Cordova received his graduate degree in chemistry from the University of California, Los Angeles. He was a founding leader of the University of California, Berkeley Global Science Institute. In 2019, he joined the Royal Scientific Society in Amman, Jordan, as executive director of Scientific Research and senior assistant to Her Royal Highness Princess Sumaya bint El Hassan for Scientific Affairs. His research focuses on developing the principles of reticular chemistry for applications in clean energy, health, and the environment.



Yue-Biao Zhang obtained both his B.Sc. and Ph.D. from Sun Yat-Sen University under the supervision of Professor Xiao-Ming Chen in 2006 and 2011, respectively. Thereafter, he worked as a postdoctoral fellow in Professor Omar M. Yaghi's group at UCLA, LBNL, and UC Berkeley. In 2015, he joined the School of Physical Science and Technology at ShanghaiTech University as an assistant professor. His research interest is novel porous materials (e.g., metal–organic frameworks, covalent organic frameworks, and zeolitic imidazolate frameworks) for sustainable technologies, such as carbon capture, methane storage, and adsorption separation.